J. Phys.: Condens. Matter **21** (2009) 124201 (8pp) doi:10.1088/0953-8984/21/12/124201

Neutron powder diffraction determination of the magnetic structure of $Gd_3Ag_4Sn_4$

J M Cadogan[1], D H Ryan[2], M Napoletano[3], P Riani[3] and L M D Cranswick[4]

[1] Department of Physics and Astronomy, University of Manitoba, Winnipeg, MB, R3T 2N2, Canada
[2] Department of Physics, McGill University, Montreal, QC, H3A 2T8, Canada
[3] Dipartimento di Chimica e Chimica Industriale, Università degli Studi di Genova, Via Dodecaneso 31, 16146 Genova, Italy
[4] Canadian Neutron Beam Centre, NRCC, Chalk River Laboratories, Chalk River, ON, K0J 1J0, Canada

E-mail: cadogan@physics.umanitoba.ca

Received 9 October 2008, in final form 6 November 2008
Published 25 February 2009
Online at stacks.iop.org/JPhysCM/21/124201

Abstract

Natural gadolinium is the strongest neutron-absorbing element and neutron diffraction studies of Gd-containing materials rely on the use of either enriched Gd isotopes or short neutron wavelengths where the absorption is weaker but, unfortunately, the neutron flux is also weak. We have employed a new sample-mounting technique to obtain neutron powder diffraction patterns from the intermetallic compound $Gd_3Ag_4Sn_4$ containing natural Gd, at a neutron wavelength of ~ 2.37 Å where there is much greater flux. Here, we report the magnetic structure of $Gd_3Ag_4Sn_4$. The magnetic ordering temperature is 28.8(2) K. At 2.8 K the Gd(4e) sublattice is antiferromagnetically ordered along the crystal c-axis, commensurate with the crystal lattice. The Gd(2d) sublattice is also ordered along the c-axis but its magnetic structure is incommensurate with the crystal lattice.

(Some figures in this article are in colour only in the electronic version)

1. Introduction

The $R_3T_4X_4$ family (R = rare earth, T = Cu, Ag, Au, and X = Si, Ge, Sn) is an extensive series of isostructural compounds which exhibit a rich variety of magnetic ordering. They crystallize in the orthorhombic $Gd_3Cu_4Ge_4$-type structure (space group *Immm*, #71) [1] in which the R atoms occupy two crystallographic sites (2d and 4e), the T atoms occupy the 8n site and the X atoms occupy two equi-populous sites (4f and 4h). In general, the R moments order antiferromagnetically, often with quite different moment values and with distinct magnetic structures adopted by the two R sublattices. In some cases the two R sublattices will also have quite different ordering temperatures and we refer the reader to our recent review of the magnetism of the $R_3T_4X_4$ compounds [2] for further details.

The magnetism of $Gd_3Ag_4Sn_4$ was first studied by Mazzone *et al* [3] who observed magnetic 'events' at 22 K and 8 K in ac-susceptibility measurements. The 22 K 'event' could be suppressed by an applied field of 1 T and the magnetization curve, obtained at 5 K, suggested a purely antiferromagnetic ordering of the Gd sublattices.

Voyer *et al* [4] used ^{119}Sn Mössbauer spectroscopy to show that the magnetic ordering temperature of $Gd_3Ag_4Sn_4$ is in fact 28.8(2) K. The Sn atoms are non-magnetic and act as a probe of their local magnetic environment i.e. the magnetic order of the Gd sublattices. The ^{119}Sn spectra comprise two equal-area magnetic sextets and the dramatic changes at $\sim$8 K in the temperature dependences of the transferred hyperfine fields at the two Sn sites were interpreted as indicating that the 8 K 'event' observed by Mazzone *et al* [3] is actually a spin-reorientation of the Gd magnetic order, rather than a magnetic ordering of one of the Gd sublattices. The changes in the electric quadrupole shift at the ^{119}Sn nuclei (by about a factor of -2) are consistent with this interpretation.

In previous studies of the $R_3T_4X_4$ series and other R–T intermetallic series, we have demonstrated the extremely productive complementarity of Mössbauer spectroscopy (a

local probe) and neutron diffraction (an *extended* probe) [5, 6]. In this context it would be desirable to carry out a neutron powder diffraction study of $Gd_3Ag_4Sn_4$ to complement our previous ^{119}Sn Mössbauer work.

Neutron diffraction is by far the best means of determining magnetic structures. However, studies of Gd-containing materials are scarce due to the fact that natural Gd is the strongest neutron-absorbing element in the periodic table. The absorption cross-section of natural Gd is 49 700 b at a neutron wavelength of 1.80 Å, an overwhelming factor of 20 times greater than that of Cd (2520 b), a widely used neutron shielding material [7]! The neutron absorption by natural Gd is a consequence of nuclear resonances in ^{155}Gd and ^{157}Gd and the neutron scattering studies carried out to date employed Gd which had been enriched in isotopes such as ^{160}Gd where the neutron absorption is much weaker. Naturally, such samples carry a financial penalty due to the isotopic enrichment.

Neutron absorption in Gd is also strongly energy-dependent [8] and the absorption cross-section decreases rapidly with increasing neutron energy (decreasing λ), reaching about 35 000 b by $\lambda = 1.33$ Å, still highly absorbing. By $\lambda \sim 0.5$ Å the absorption cross-section is a manageable few hundred b. However, at such short neutron wavelengths the thermal neutron flux from a reactor is quite low, leading to greatly increased counting times. Furthermore, the use of such a short neutron wavelength compresses the powder diffraction pattern into a narrower, lower scattering angle (2θ) range than is optimum for resolution and pattern refinement considerations.

Recently, two of us reported a new method for obtaining usable quality diffraction patterns from samples containing natural Gd and at neutron wavelengths close to the peak in the thermal distribution [9]. Basically, we use a flat-plate sample holder with silicon single-crystal windows in which the powder sample is thinly spread and covers a significant area of the incident beam, effectively turning the powder into a 'thin film'. The increased 'beam coverage' compensates for the thin sample. In this way, we can obtain reasonable quality magnetic diffraction patterns at $\lambda \sim 2.37$ Å, which allows us to spread the magnetic peaks to higher angles than in the case of $\lambda \sim 0.5$ Å, thereby improving the resolution of the magnetic peaks, as mentioned above.

In this paper we present neutron powder diffraction measurements we recently made on the intermetallic compound $Gd_3Ag_4Sn_4$. The quality of the diffraction patterns obtained using our new sample-mounting technique is sufficient to allow us to determine the magnetic structures of the two Gd sublattices in $Gd_3Ag_4Sn_4$. We are able to identify the ordering modes for the two Gd sites and also show that our neutron diffraction results are consistent with our previous ^{119}Sn Mössbauer work. In particular, we can confirm that $Gd_3Ag_4Sn_4$ undergoes a spin-reorientation at ~8 K from the ab-plane to the c-axis upon cooling.

2. Experimental methods

The $Gd_3Ag_4Sn_4$ sample was prepared by arc melting stoichiometric amounts of the pure elements (Gd 99.9 wt%, Ag and Sn 99.999 wt%). The arc-melted ingot was turned and remelted several times in order to ensure homogeneity. The alloyed button was then sealed under vacuum in a quartz tube, annealed for 20 days at 873 K and quenched in water. Cu Kα x-ray diffraction and electron microprobe analysis confirmed the majority phase to be the intended orthorhombic $Gd_3Ag_4Sn_4$ phase. Refinement of the x-ray diffraction pattern using the GSAS/EXPGUI package [10, 11] showed the presence of less than 2 wt% of the ζ-phase $Ag_{79}Sn_{21}$. Basic magnetic characterization was carried out on a Quantum Design PPMS susceptometer/magnetometer.

Neutron diffraction experiments were carried out on the C2 multi-wire powder diffractometer (DUALSPEC) at the NRU reactor, Canadian Neutron Beam Centre, Chalk River, Ontario. The neutron wavelength was 2.372 11(16) Å. The extreme absorption cross-section of natural Gd leads to a $1/e$ thickness of about 14 μm for $Gd_3Ag_4Sn_4$ at the wavelength used here. Approximately 300 mg of the $Gd_3Ag_4Sn_4$ compound was spread on a 600 μm single-crystal silicon plate, to cover an area of 8 cm by 2.4 cm, and immobilized using highly diluted (1% by wt) GE-7031 varnish [9]. The plate was oriented with its surface normal parallel to the incident neutron beam in order to maximize the total flux onto the sample.

Temperatures down to 2.8 K were obtained using a closed-cycle refrigerator. The diffraction data were obtained in a series of interleaved temperature runs rather than as a single time/temperature series. This allowed us to separate time-dependent artefacts from genuine temperature dependences, a strategy that is essential when dealing with such weak scattering signals.

All refinements of the neutron diffraction patterns employed the FullProf/WinPlotr suite [12, 13] and the magnetic structures were drawn using the FP-Studio package, part of the FullProf/WinPlotr suite. No absorption correction was applied, however the data were truncated at $2\theta = 60°$ to minimize the impact of angle-dependent absorption effects. The limited Q-range considered ($Q < 2.65$ Å^{-1}) and the low measurement temperatures used ($T < 35$ K) greatly limit the effects of atomic vibrations on the observed diffraction patterns and so all thermal factors were set to zero.

3. Results and discussion

3.1. Basic characterization

The x-ray powder diffraction pattern of $Gd_3Ag_4Sn_4$ obtained at room temperature confirms the formation of the orthorhombic $Gd_3Cu_4Ge_4$-type structure. The refined lattice parameters are $a = 15.2068(4)$ Å, $b = 7.2995(2)$ Å and $c = 4.5602(1)$ Å, in good agreement with a recent study by Romaka *et al* [14]. We note here that our lattice setting (i.e. $a > b > c$) differs from that used by Romaka *et al* ($a < b < c$) so the specific site notations are different. In table 1 we give the refined atomic position parameters of $Gd_3Ag_4Sn_4$, deduced from the refinement of the x-ray powder diffraction pattern.

In figure 1 we show the magnetization curves of $Gd_3Ag_4Sn_4$ obtained over the temperature range 5–25 K, in applied magnetic fields up to 2 T. The behaviour is

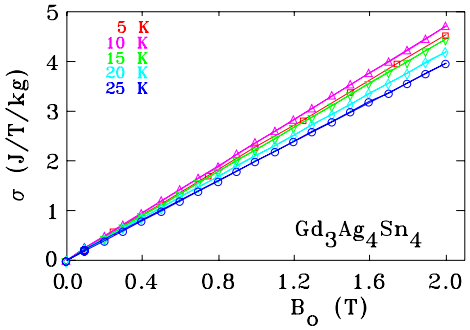

Figure 1. Magnetization curves of $Gd_3Ag_4Sn_4$ at various temperatures in the range 5–25 K and in applied magnetic fields up to 2 T.

Table 1. Crystallographic data for $Gd_3Ag_4Sn_4$ obtained by refinement of the room-temperature x-ray powder diffraction pattern (Cu Kα).

Atom	Site	x	y	z
Gd	2d	$\frac{1}{2}$	0	$\frac{1}{2}$
Gd	4e	0.1284(1)	0	0
Ag	8n	0.3291(2)	0.1994(2)	0
Sn	4f	0.2151(3)	$\frac{1}{2}$	0
Sn	4h	0	0.1962(2)	$\frac{1}{2}$

characteristic of an antiferromagnetic ordering of the Gd sublattices with no sign of any ferromagnetic components in the magnetic structure. One interesting feature is the fact that the magnetization at 10 K is slightly higher than that at 5 K. This may be a sign of orbital effects associated with a spin-reorientation (*vide infra*). Although Gd^{3+} is an S-state ion, it is not completely impervious to the effects of anisotropy, as a consequence of dipole effects [15].

3.2. Scattering length

Before discussing the refinement of the neutron diffraction patterns, we must consider the neutron scattering length for natural Gd. The scattering length is a complex quantity which is dominated by an imaginary term arising from the aforementioned nuclear resonances. The scattering length is strongly dependent on the neutron energy (E) and has been documented by Lynn and Seeger [8]. To determine the scattering length components appropriate to our neutron wavelength ($\lambda = 2.372\,11$ Å and $E = 14.54$ meV) we fitted the Lynn and Seeger data with cubic polynomials, up to $E = 40$ meV. The values of the real and imaginary components of the scattering length of natural gadolinium, for our neutron wavelength, are 3.0 fm and −12.7 fm, respectively.

4. Neutron powder diffraction

In figure 2 we show a comparison of the neutron powder diffraction patterns we obtained on $Gd_3Ag_4Sn_4$. The sharp feature in some of the patterns at $2\theta \sim 27°$ was identified as an artefact by comparing data taken at different times but at the same temperature. It was found to be present in a consistent block of time that correlated with maintenance work being done on the reactor, but did not show a consistent temperature association. This artefact was therefore removed from all patterns used in the analysis that follows.

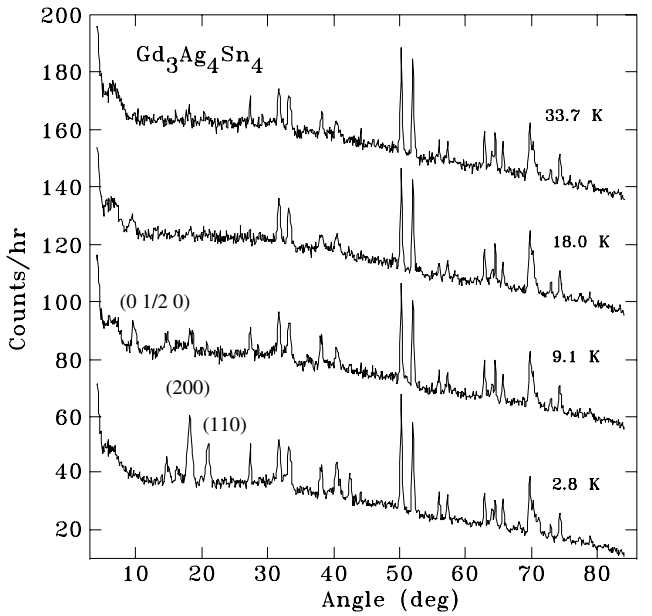

Figure 2. Neutron diffraction patterns of $Gd_3Ag_4Sn_4$ obtained with a neutron wavelength of $\lambda = 2.372\,11(16)$ Å.

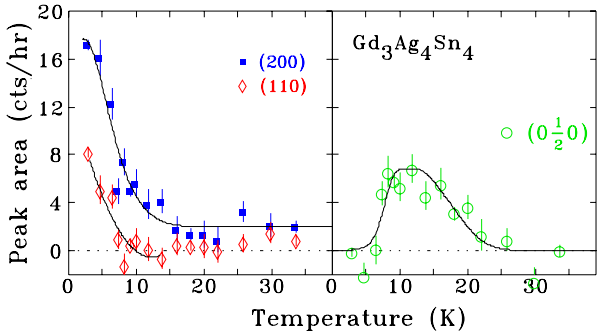

Figure 3. Temperature dependences of the (200), (110) and (0 $\frac{1}{2}$ 0) peak areas of $Gd_3Ag_4Sn_4$.

Despite the somewhat poor signal to noise ratio, the effects of the magnetic ordering of the Gd sublattices are clear, in particular in the 2θ range 12°–22°. The three principal magnetic contributions are indexed as (0 $\frac{1}{2}$ 0), (200) and (110), as indicated in figure 2, and in order to follow the development of the magnetic order in $Gd_3Ag_4Sn_4$ we show in figure 3 the temperature dependences of the integrated areas of the (200), (110) and (0 $\frac{1}{2}$ 0) peaks. The (0 $\frac{1}{2}$ 0) peak appears at the magnetic ordering temperature and reaches its maximum intensity at around 12 K. At around 8–9 K the intensity of this purely magnetic peak decreases sharply and this peak disappears by about 7 K. Consistent with this behaviour, we see substantial increases in the intensities of both the (200) and (110) peaks, starting at around 12 K. These latter two peaks contain both nuclear and magnetic contributions.

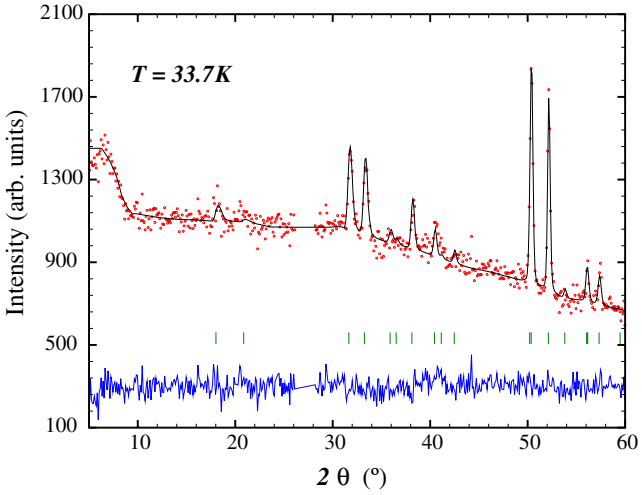

Figure 4. Refined neutron diffraction pattern of $Gd_3Ag_4Sn_4$, obtained at 33.7 K. The Bragg markers represent the nuclear scattering from the $Gd_3Ag_4Sn_4$ crystal structure.

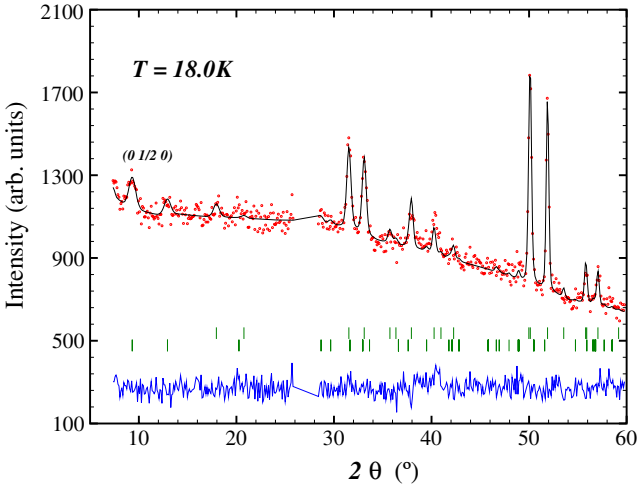

Figure 5. Refined neutron diffraction pattern of $Gd_3Ag_4Sn_4$, obtained at 18.0 K. The Bragg markers represent the nuclear (top) and magnetic (bottom) scattering.

In this section we will give a brief qualitative description of the main magnetic features in our diffraction patterns and in the following section we will present a more quantitative analysis of the patterns, based on representational analysis, leading to the determination of the magnetic structures of the two Gd sublattices in $Gd_3Ag_4Sn_4$.

4.1. 33.7 K pattern

At 33.7 K, $Gd_3Ag_4Sn_4$ is paramagnetic and the neutron diffraction pattern is purely nuclear. Using the complex scattering length determined above, we obtained the refinement to the crystal structure shown in figure 4. The refined lattice parameters at 33.7 K are $a = 15.1586(4)$ Å, $b = 7.2684(2)$ Å and $c = 4.5434(1)$ Å. These parameters are reduced by 0.32%–0.43% relative to the room-temperature values.

4.2. 18.0 K pattern

As mentioned earlier, our previous ^{119}Sn Mössbauer work [4] gave a magnetic ordering temperature of 28.8(2) K, with no indications of independent ordering of the two Gd sublattices. The neutron powder diffraction pattern obtained at 18.0 K therefore comprises both nuclear and magnetic contributions and is shown in figure 5.

The only clear signal of magnetic ordering in the 18.0 K pattern is the peak at $2\theta = 9.3°$. This peak indexes as $(0\ \frac{1}{2}\ 0)$, indicating that the magnetic ordering of *at least* one of the Gd sublattices involves a cell-doubling along the crystal *b*-axis, i.e. a propagation vector $\mathbf{k}_1 = [0\ \frac{1}{2}\ 0]$. Needless to say, we cannot be specific about the actual magnetic structure of $Gd_3Ag_4Sn_4$ at 18.0 K on the basis of a single, albeit purely magnetic peak. However, as we shall show in section 5, we believe that the $(0\ \frac{1}{2}\ 0)$ peak is due to ordering of the Gd(4e) sublattice and we refined the 18.0 K diffraction pattern accordingly. The value of the Gd(4e) magnetic moment at 18.0 K is 4.9 μ_B.

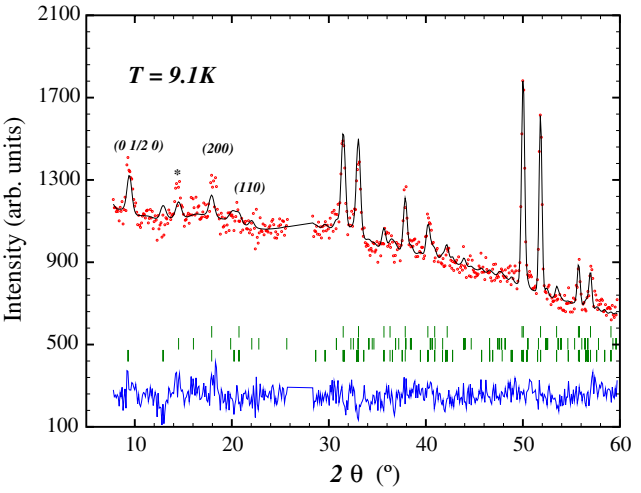

Figure 6. Refined neutron diffraction pattern of $Gd_3Ag_4Sn_4$, obtained at 9.1 K. The Bragg markers are (top) nuclear phase, (middle) Gd(2d) magnetism and (bottom) Gd(4e) magnetism. An incommensurate peak is marked with an asterisk.

4.3. 9.1 K pattern

Inspection of the diffraction patterns in figure 2 shows a number of clear peaks resulting from the magnetic contribution at 9.1 K. The $(0\ \frac{1}{2}\ 0)$ peak, observed at 18.0 K, is stronger and there are also clear magnetic contributions to nuclear peaks, in particular the (200) peak and, to a lesser extent the (110) peak, at $2\theta = 17.9°$ and $2\theta = 20.8°$ respectively. These contributions correspond to a propagation vector $\mathbf{k}_2 = [0\ 0\ 0]$. There are also two weak incommensurate peaks on the low-angle side of the (200) peak (marked with asterisks in the neutron diffraction figures). The importance of these incommensurate peaks will be outlined in the following section. The refined neutron powder diffraction pattern obtained at 9.1 K is shown in figure 6.

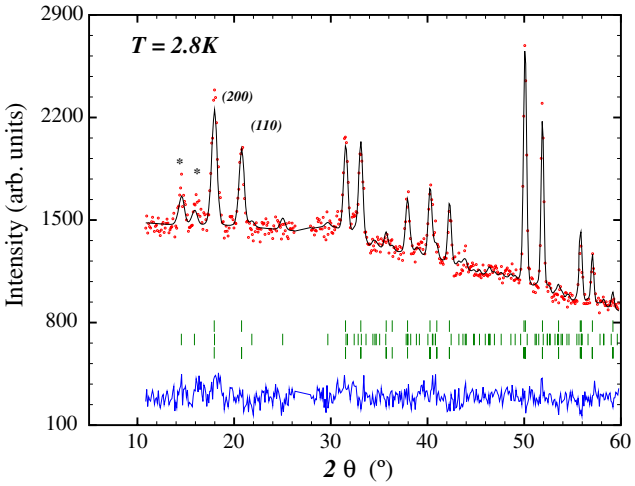

Figure 7. Refined neutron diffraction pattern of $Gd_3Ag_4Sn_4$, obtained at 2.8 K. The Bragg markers are (top) nuclear phase, (middle) Gd(2d) magnetism and (bottom) Gd(4e) magnetism. Incommensurate peaks are marked with asterisks.

4.4. 2.8 K pattern

The magnetic contribution at 2.8 K is quite clear in the diffraction patterns shown in figure 2. Besides the $\mathbf{k}_2 = [0\ 0\ 0]$ magnetic contributions to (200) and (110) we also see additional, purely magnetic peaks, two of which are quite prominent on the lower-angle side of the (200) peak (marked with asterisks in figure 7 and appearing at $2\theta = 14.5°$ and 16.0°). These two peaks are incommensurate with the $Gd_3Ag_4Sn_4$ crystal lattice and are also present in the 9.1 K pattern, as mentioned above.

Given that there are two Gd magnetic sublattices in $Gd_3Ag_4Sn_4$ and clear magnetic contributions at *both* commensurate and incommensurate positions in the 2.8 K diffraction pattern we can associate one Gd site with the commensurate magnetic order and the other site with the incommensurate magnetic order. The obvious question is now whether we can be specific as to which site is which.

5. Magnetic order

In this section we will present a detailed description of the refinements to the diffraction patterns of $Gd_3Ag_4Sn_4$, based on representational analysis.

5.1. Commensurate magnetic order

Taking into account the weak nuclear contributions to the prominent (200) and (110) peaks, we estimate the ratio of the (200)/(110) magnetic contributions to be 1.8(3) at 2.8 K. To identify the site responsible for these commensurate magnetic contributions we carried out representational analysis for each Gd site (2d and 4e) using the SARA*h* program [16].

Representational analysis for the Gd(2d) site with a propagation vector [0 0 0] shows that the decomposition of the magnetic representation comprises three one-dimensional representations:

$$\Gamma^{2d}_{\mathrm{Mag}} = 1\Gamma^{(1)}_3 + 1\Gamma^{(1)}_5 + 1\Gamma^{(1)}_7 \quad (1)$$

using the notation employed in SARA*h*. The basis vectors of these irreducible representations are given in table 2.

Representational analysis for the Gd(4e) site, with a propagation vector [0 0 0], shows that the decomposition of the magnetic representation comprises six one-dimensional representations:

$$\Gamma^{4e}_{\mathrm{Mag}} = 1\Gamma^{(1)}_2 + 1\Gamma^{(1)}_3 + 1\Gamma^{(1)}_5 + 1\Gamma^{(1)}_6 + 1\Gamma^{(1)}_7 + 1\Gamma^{(1)}_8 \quad (2)$$

and the basis vectors of these irreducible representations are given in table 3.

The only allowed ordering directions with $\mathbf{k}_2 = [0\ 0\ 0]$ are along the crystal axes for both the Gd(2d) and Gd(4e) sublattices. We can estimate the (200)/(110) ratio of magnetic contributions at 2.8 K for both Gd sites, assuming a moment of 7 μ_B on the Gd (a reasonable assumption given the S-state nature of the Gd^{3+} ion.) In tables 2 and 3 we give the (200)/(110) magnetic ratios obtained from simulations using FullProf [12]. The best match to the observed intensity ratio is with the Gd(4e) sites ordered antiferromagnetically (+ −) along the crystal *c*-axis, corresponding to the $\Gamma^{(1)}_6$ representation (figure 8). The magnitude of the Gd(4e) magnetic moment at 2.8 K is 6.8 μ_B.

In figure 7 we show the refinement to the neutron diffraction pattern obtained at 2.8 K. The Gd(2d) order is incommensurate and will be discussed below.

Table 2. Representational analysis for the Gd(2d) site in $Gd_3Ag_4Sn_4$ with a propagation vector [0 0 0]. The atomic position of the primitive basis is $(\frac{1}{2},\ 0,\ \frac{1}{2})$.

Representation	Basis vector	Atom 1 order	Magnetic ratio (200)/(110)
$\Gamma^{(1)}_3$	ψ_1	[1 0 0]	0
$\Gamma^{(1)}_5$	ψ_2	[0 1 0]	3.65
$\Gamma^{(1)}_7$	ψ_3	[0 0 1]	0.68

Table 3. Representational analysis for the Gd(4e) site in $Gd_3Ag_4Sn_4$ with a propagation vector [0 0 0]. The atomic positions defining the non-primitive basis are $(x,\ 0,\ 0)$ and $(-x,\ 0,\ 0)$.

Representation	Basis vector	Atom 1 order	Atom 2 order	Magnetic ratio (200)/(110)
$\Gamma^{(1)}_2$	ψ_1	[1 0 0]	$[\bar{1}\ 0\ 0]$	0
$\Gamma^{(1)}_3$	ψ_2	[1 0 0]	[1 0 0]	0
$\Gamma^{(1)}_5$	ψ_3	[0 1 0]	[0 1 0]	0.05
$\Gamma^{(1)}_6$	ψ_4	[0 0 1]	$[0\ 0\ \bar{1}]$	1.25
$\Gamma^{(1)}_7$	ψ_5	[0 0 1]	[0 0 1]	0.01
$\Gamma^{(1)}_8$	ψ_6	[0 1 0]	$[0\ \bar{1}\ 0]$	6.72

5.2. Doubled magnetic order

The presence of a purely magnetic $(0\ \frac{1}{2}\ 0)$ peak in the temperature range 9–28 K, whose disappearance coincides

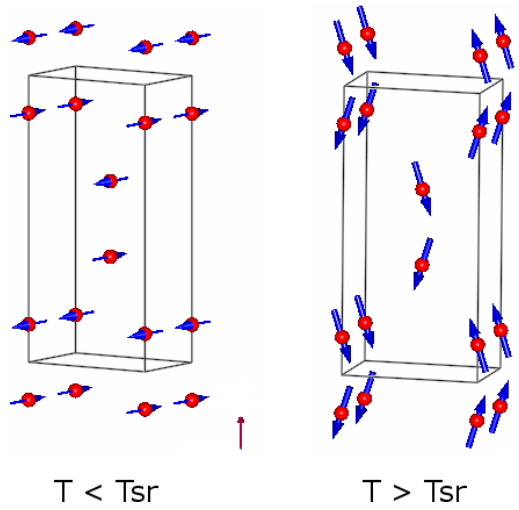

Figure 8. Magnetic structures of the Gd(4e) sublattice in $Gd_3Ag_4Sn_4$ below and above the spin-reorientation temperature (T_{sr}). The view is of the *ab*-plane, tilted slightly. The *a*-axis is vertical, as indicated by the arrow.

Table 4. Representational analysis for the Gd(4e) site in $Gd_3Ag_4Sn_4$ with a propagation vector [0 $\frac{1}{2}$ 0]. The atomic positions defining the non-primitive basis are (x, 0, 0) and ($-x$, 0, 0).

Representation	Basis vector	Atom 1 order	Atom 2 order
$\Gamma_1^{(1)}$	ψ_1	[0 0 1]	[0 0 $\bar{1}$]
$\Gamma_2^{(1)}$	ψ_2	[1 0 0]	[$\bar{1}$ 0 0]
$\Gamma_2^{(1)}$	ψ_3	[0 1 0]	[0 1 0]
$\Gamma_3^{(1)}$	ψ_4	[1 0 0]	[1 0 0]
$\Gamma_3^{(1)}$	ψ_5	[0 1 0]	[0 $\bar{1}$ 0]
$\Gamma_4^{(1)}$	ψ_6	[0 0 1]	[0 0 1]

Table 5. Representational analysis for the Gd(2d) site in $Gd_3Ag_4Sn_4$ with a propagation vector $\mathbf{k}$ = [0.43, 0.19, 0].

Representation	Basis vector	Atom 1 order
$\Gamma_1^{(1)}$	ψ_1	[0 0 1]
$\Gamma_2^{(1)}$	ψ_2	[1 0 0]
$\Gamma_2^{(1)}$	ψ_3	[0 1 0]

with the development of substantial magnetic contributions to the (200) and (110) peaks, suggests that the doubling involves the Gd(4e) site. The fact that the two incommensurate peaks mentioned earlier in the discussion of the 2.8 K pattern are also present in the 9.1 K pattern, along with the (0 $\frac{1}{2}$ 0) peak, provides further support for the assumption that the (0 $\frac{1}{2}$ 0) peak is associated with the magnetic order of the Gd(4e) sites.

Representational analysis for the Gd(4e) site, with a propagation vector [0 $\frac{1}{2}$ 0], shows that the decomposition of the magnetic representation comprises four one-dimensional representations, two of which appear twice:

$$\Gamma_{\text{Mag}}^{4e} = 1\Gamma_1^{(1)} + 2\Gamma_2^{(1)} + 2\Gamma_3^{(1)} + 1\Gamma_4^{(1)} \quad (3)$$

and the basis vectors of these irreducible representations are given in table 4.

Representational analysis shows that the Gd(4e) magnetic moments in the doubled structure are either along the crystal *c*-axis or are in the *ab*-plane. We can rule out the Γ_1^{4e} axial representation and also the Γ_2^{4e} planar representation since they give zero intensity at (0 $\frac{1}{2}$ 0).

The best match to the observed (0 $\frac{1}{2}$ 0) intensity at 9.1 K is with the Gd(4e) sites ordered according to the Γ_3^{4e} planar representation (figure 8). Given the statistics of the pattern, we cannot be definitive about this. However, the refined magnetic moment of Gd(4e) for the Γ_3^{4e} planar representation is 5.6 μ_B compared with a value of 4.8 μ_B for the other Gd(4e) option i.e. the Γ_4^{4e} axial representation. The Gd(4e) magnetic moment makes an angle of about 20° with the crystal *a*-axis.

We can estimate the expected temperature dependence of the Gd magnetic moment using a simple $J = \frac{7}{2}$ Brillouin function. Considering only magnetic exchange effects, the observed ordering temperature of 28.8 K corresponds to a molecular field ($T = 0$) of 15 T at the Gd^{3+} ion. So, at 9 K we would expect a Gd moment of about 6.4 μ_B. At 18.0 K we would expect 5.0 μ_B. The fact that the refinement of the 9.1 K pattern using a planar magnetic configuration gives a larger Gd(4e) moment than the axial magnetic configuration is consistent with these simple exchange considerations, although not a robust verification.

5.3. Incommensurate magnetic order

Following the arguments presented in preceding sections, we attribute the presence of purely magnetic incommensurate peaks in the temperature range 3–12 K to the Gd(2d) site. Apart from the two clear incommensurate peaks at $2\theta = 14.5°$ and 16.0°, it is difficult to identify other incommensurate peaks unambiguously, although some well defined, commensurate peaks exhibit 'shoulders' which we attribute to the incommensurate magnetic phase. A tentative search for a suitable propagation vector to describe the incommensurate magnetic order of the Gd(2d) sublattice was carried out using the program *k_search*, part of the FullProf/WinPlotr package [12, 13]. One possible solution is $\mathbf{k}$ = [0.43, 0.19, 0].

Representational analysis for the Gd(2d) site with a propagation vector $\mathbf{k}$ = [0.43, 0.19, 0], shows that the decomposition of the magnetic representation comprises two one-dimensional representations, one of which occurs twice:

$$\Gamma_{\text{Mag}}^{2d} = 1\Gamma_1^{(1)} + 2\Gamma_2^{(1)}. \quad (4)$$

The corresponding basis vectors are shown in table 5.

The refinement of the 2.8 K pattern yields a magnetic structure of the Gd(2d) sublattice in $Gd_3Ag_4Sn_4$ which is described by the basis vector ψ_1 belonging to the $\Gamma_1^{(1)}$ irreducible representation. The Gd(2d) moments are aligned along the crystal *c*-axis at 2.8 K. The amplitude of the Gd(2d) magnetic moment at 2.8 K is 6.5 μ_B. The modulation of the incommensurate magnetism of the Gd(2d) sublattice is either sinusoidal or square-wave. Unfortunately, the quality of the diffraction patterns renders the observation of higher

harmonics of the propagation vector, which would resolve this issue, out of the question. However, the fact that the ^{119}Sn Mössbauer spectra reported earlier [4] show no undue broadening of the magnetic sextets, which would be expected if the magnitudes of the Gd(2d) moments were sinusoidally modulated, favours a square-wave modulation.

In figure 8 we show the magnetic structure of the Gd(4e) sublattice both below the spin-reorientation temperature ($T_{sr} \sim 8$ K) and above. As explained in the text, the determination of the Gd(2d) order is not as definitive as the Gd(4e) order so the Gd(2d) order is not shown in figure 8.

6. ^{119}Sn Mössbauer work

Our previously published ^{119}Sn Mössbauer work on $Gd_3Ag_4Sn_4$ [4] showed clearly that the magnetic ordering temperature is 28.8(2) K. Curiously, no sign of this magnetic ordering was observed by ac-susceptibility [3]. This failing on the part of ac-susceptibility seems to be a common feature of the $R_3T_4X_4$ compounds [2]. No sign of the previously reported 22 K 'event' [3] was observed by Mössbauer spectroscopy.

The temperature dependences of the hyperfine fields at the two Sn sites in $Gd_3Ag_4Sn_4$, shown in [4], exhibit clear changes at around 8 K. The Sn site with the larger hyperfine field shows a 10% drop in field at 8 K whereas the other Sn site shows an increase of almost 50%. These dramatic changes in the hyperfine fields at the two Sn sites are most likely due to the loss of the Gd(4e) contributions to the transferred hyperfine fields at the Sn sites below the spin-reorientation while additional effects from anisotropic hyperfine fields [17, 18] may also play a role as the ordering axis changes by 90°. The corresponding electric quadrupole shifts [4] show changes by about a factor of -2 upon cooling through 8 K.

The $Gd_3Ag_4Sn_4$ structure contains two Sn sites, the 4f and 4h, and each contributes a magnetically-split component to the overall ^{119}Sn Mössbauer spectrum. At 1.6 K, the ^{119}Sn spectrum comprises two magnetic sextets with equal areas. The ratio of the transferred hyperfine fields at the two Sn sites is 2.08:1. As outlined in our paper on $Dy_3Ag_4Sn_4$ [6], the X(4f) site in the $R_3T_4X_4$ structure has one R(2d) and four R(4e) nearest-neighbours while the X(4h) site has two R(2d) and four R(4e) nearest-neighbours. The magnetic structures of the Dy sublattices in $Dy_3Ag_4Sn_4$ led to a splitting of one of the ^{119}Sn Mössbauer components, yielding three magnetic sextets in the area ratio 2:1:1. This provided a useful verification of the results of our refinement of the neutron diffraction pattern.

As shown in section 5, the Gd(4e) sublattice is ordered antiferromagnetically along the crystal *c*-axis at 2.8 K. Summation of the transferred hyperfine fields at each of the eight Sn sites in this structure (4f and 4h) shows that the *net* contribution of the Gd(4e) magnetic order to the ^{119}Sn transferred hyperfine field at 2.8 K is zero at all Sn sites. Thus, the observed transferred fields at the Sn sites at 2.8 K arise from the Gd(2d) order. A simple estimate of the ratio of the transferred hyperfine fields is 2:1, i.e. the ratio of the number of Gd(2d) nearest-neighbours at the two Sn sites, allowing us to identify the Sn site having the larger hyperfine field as the 4h site.

To a first approximation, the electric quadrupole shift of a Mössbauer spectrum, in the presence of a magnetic field, involves an angular term $(3\cos^2\theta - 1)$, where θ is the angle between the hyperfine field and the principal axis of the electric field gradient at the ^{119}Sn nucleus. A reorientation of the Gd magnetic order (and hence the transferred hyperfine field at the ^{119}Sn nucleus) is evident in the temperature dependence of the electric quadrupole shifts. The change by about a factor of -2 is consistent with a 90° reorientation of the magnetic order, as suggested in our earlier paper [4].

Our neutron diffraction work shows that the magnetic order of the Gd(4e) sublattice does indeed undergo a 90° reorientation from planar to axial upon cooling. In the planar structure, there is a net transferred hyperfine field at the Sn sites from the Gd(4e) sublattice, in addition to the contribution from the Gd(2d) sublattice. The ratio of the two ^{119}Sn hyperfine fields is closer to 3:1 at temperatures just above the spin-reorientation, as a result. The Gd(2d) sublattice magnetic order is *c*-axial at 2.8 K, i.e. collinear with the Gd(4e) order. The magnetic ordering temperature of $Gd_3Ag_4Sn_4$ is 28.8(2) K and it is conceivable that this exchange is sufficient to keep the two Gd sublattices collinear, particularly in light of the expected weak anisotropy of the Gd^{3+} sublattice magnetizations. Thus, the Gd(2d) would also undergo a 90° reorientation from planar to axial. This would be fully consistent with our ^{119}Sn Mössbauer work but we are unable to provide definitive proof of this suggestion yet.

7. Future upgrades—Quo Vadis?

While the quality of the diffraction patterns presented here does limit the conclusions that can be reached, it is clear that it is now possible to obtain useful neutron scattering data on compounds containing a significant amount of natural gadolinium. Moreover, our diffraction data have been obtained at relatively long wavelengths (~2.37 Å) where well-resolved magnetic scattering is observed. Several upgrades to the C2 diffractometer at Chalk River are currently underway. The re-installation of the D_2O scattering can for the C2 beam-line and the monochromator upgrade should both be completed by mid-2009, while construction of a new ^{3}He-filled multi-wire detector is projected for the end of 2010. Collectively, these should improve the instrument figure of merit by about a factor of ten, reducing the counting time needed and greatly improving the data quality that can be expected for highly-absorbing samples. Even now, there are several facilities world-wide that could adopt these flat-plate-mounting procedures [9] for work with natural gadolinium compounds.

8. Conclusions

We have determined the magnetic structure of $Gd_3Ag_4Sn_4$ by neutron powder diffraction using our new flat-plate technique for obtaining diffraction patterns from highly-absorbing samples. The magnetic ordering temperature is 28.8(2) K. At 2.8 K, the magnetic order of the Gd(4e) sublattice is commensurate with the crystal lattice. The Gd(4e)

moments are aligned antiferromagnetically along the *c*-axis. The magnetic order of the Gd(2d) sublattice is incommensurate at 2.8 K, with the Gd moments also aligned along the *c*-axis. Our diffraction data suggest that the magnetic 'event' previously observed at ∼8 K, is a 'plane to axis' spin-reorientation of the Gd magnetic structure upon cooling. This is consistent with our previous ^{119}Sn Mössbauer spectroscopy work.

Acknowledgments

It is a great pleasure to acknowledge here the extensive contributions that Dr Trevor Hicks has made to the science of neutron scattering, in general, and to the practice of this fine art in Australia, in particular. JMC and DHR were introduced to neutron scattering on Trevor's LONGPOL spectrometer at the HIFAR reactor in Sydney.

JMC and DHR are grateful to the staff of the CNBC, Chalk River, for their open approach to new ideas, their active support and encouragement during the development of the flat-plate sample mounts, and the extensive technical and scientific support provided during the course of the neutron diffraction measurements presented here.

JMC acknowledges support from the Canada Research Chairs scheme. Financial support for various stages of this work was provided by the Natural Sciences and Engineering Research Council of Canada and Fonds Québécois de la Recherche sur la Nature et les Technologies.

Finally, JMC is grateful to Dr Andrew Wills and Dr Juan Rodríguez-Carvajal for enlightening discussions.

References

[1] Rieger W 1970 *Monatsch. Chem.* **101** 449–62
[2] Ryan D H, Cadogan J M, Voyer C, Napoletano M, Riani P and Cranswick L M D 2008 *Hyperfine Interact.* at press
[3] Mazzone D, Riani P, Napoletano M and Canepa F 2005 *J. Alloys Compounds* **387** 15–9
[4] Voyer C J, Ryan D H, Napoletano M and Riani P 2007 *J. Phys.: Condens. Matter* **19** 156209
[5] Ryan D H, Cadogan J M, Gagnon R and Swainson I P 2004 *J. Phys.: Condens. Matter* **16** 3183–98
[6] Perry L K, Cadogan J M, Ryan D H, Canepa F, Napoletano M, Mazzone D and Riani P 2006 *J. Phys.: Condens. Matter* **18** 5783–92
[7] Sears V F 1992 *Neutron News* **3** 26–37
[8] Lynn J E and Seeger P A 1990 *At. Data Nucl. Data Tables* **44** 191–207
[9] Ryan D H and Cranswick L M D 2008 *J. Appl. Crystallogr.* **41** 198–205
[10] Larson A C and von Dreele R B 2004 *Los Alamos National Laboratory Report* LAUR 86–748 unpublished
[11] Toby B H 2001 *J. Appl. Crystallogr.* **34** 210–21
[12] Rodríguez-Carvajal J 1993 *Physica* B **192** 55–69
[13] Roisnel T and Rodríguez-Carvajal J 2001 *Mater. Sci. Forum* **378–381** 118–23
[14] Romaka V V, Davydov V, Gladyshevskii R and Melnychenko N 2007 *J. Alloys Compounds* **443** 68–70
[15] Rotter M, Loewenhaupt M, Doerr M, Lindbaum A, Sassik H, Ziebeck K and Beuneu B 2003 *Phys. Rev.* B **68** 144418
[16] Wills A S 2000 *Physica* B **276–8** 680–1 program available from www.chem.ucl.ac.uk/people/wills/
[17] Le Caër G, Malaman B, Venturini G and Kim I B 1982 *Phys. Rev.* B **26** 5085–96
[18] Perry L K, Ryan D H and Venturini G 2007 *Phys. Rev.* B **75** 144417